International Journal of Systems Signal Control and Engineering Application 9 (5-6): 121-132, 2016
ISSN: 1997-5422

Designing a Backup Control System for Micro-Grids during Fault Condition

Seyed Sajjad Hosseini and Hesam Rahbarimagham
Department of Electrical and Computer Engineering, Rafsanjan Branch,
Islamic Azad University, Rafsanjan, Iran

Abstract: Now a days increased presence of distributed generations in distribution systems has created a new structure namely as micro-grids which include several advantages such as responsiveness towards energy demands, reliability, reduced offline times, increased efficiency and environment related arguments. Micro-grids are usually found in two types including network connected and network independent. A micro-grid's suitable performance is in debt of existence of an efficient control system since the issue of stability is considered as a crucial parameter in terms of energy management and planning in grids and micro-grids. An important component in terms of controlling micro-grids in network independent mode is micro-grid's voltage and frequency controlling. There are several strategies for doing so but the most important one is the droop method. The present study tries to benefit from a PID fuzzy controller for optimal management of behavior of the backup control system aimed at controlling the micro-grid during fault condition. Data analyses and related simulations have been performed using the matlab Software. Results regarding the PID fuzzy controller revealed a higher precision and speed in terms of neutralization of the fault compared to previous methods. The proposed controller overcomes the complexities of previous methods such as using a decision making tree. In fact the proposed controller is simpler than previous ones but yet more precise and faster.

Key words: Distributed generations, PID fuzzy, micro-grid, fuzzy logic controller, V/F controller, droop method, energy saving batteries

INTRODUCTION

Along with the advances of human communities, electricity has remained as the symbol of modern civilization. Now a days the issues of reliability and quality of power supplies have gained more importance. In addition reduced supplies in conventional sources and environmental pollutions have challenged the production of electricity from fossil fuels (Xu *et al*., 2013).

The increasing trend in consumption of energy in different contexts and also the increase of the same index in terms of electricity have increased the necessities of the need for supplication of electricity with least off-line times and highly reliable and high quality electric loads (Rahbarimagham *et al*., 2015).

Furthermore, it shouldn't be disregarded that conventionally, electricity was produced through methods including using fossil fuels. However, since these fuels impose a great deal of pollution on environment and considering the fact that the fuels themselves are becoming rarer every day; they can no longer be considered as a suitable option. As a result, researchers and scholars have been forced to improve and upgrade the conventional production methods through optimization of grids and making use of new energy production methods also known as green energy.

As a result of several universal advantages of using restructured grids, global tendencies towards these grids are rising. In addition, requiring sensitive loads by special organs such as hospitals, information centers, communication systems, etc. on the one hand and development of energy production technologies, increased importance of environmental issues, transformation of distribution grids from passive state to active, increased motivation for new energies and especially renewable energies and existing of necessary will for improvement of reliability of electrical grids on the other hand have persuaded the associates of power industries towards distributed generation and micro-grids. Existence of Renewable Energy Sources (RESs) in micro-grids helps with global warming reduction and increased pace of movement of the industry of electricity towards restructures environments (Mahmoud *et al*., 2014).

As the technologies of electricity, power and modern control theories develop and expand, micro-grids which are combinations of distributed generation, energy saving

Corresponding Author: Hesam Rahbarimagham, Department of Electrical and Computer Engineering, Rafsanjan Branch, Islamic Azad University, Rafsanjan, Iran

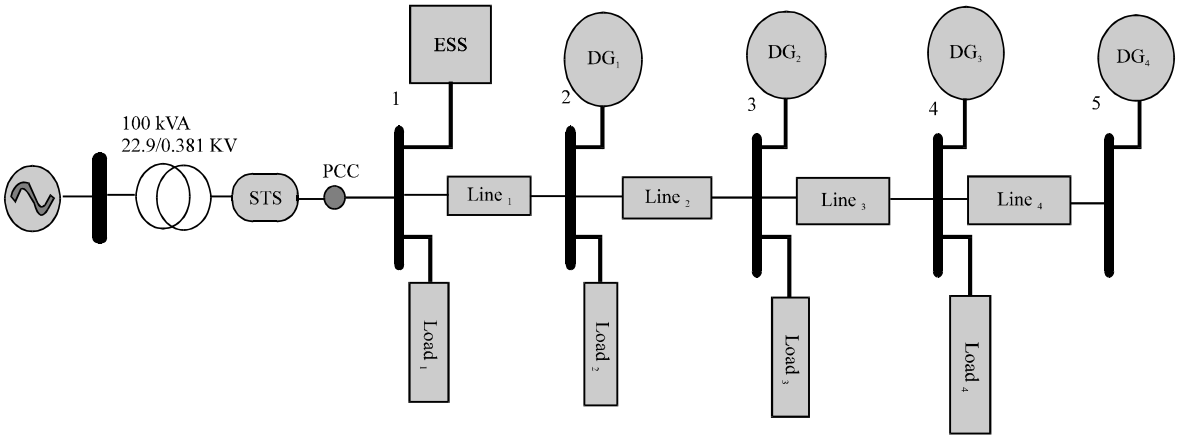

Fig. 1: Micro-grid configuration

devices, loads and control modules are rapidly being considered for promotion of responsiveness towards increased load demand. In addition, the former provide a solution for obtaining distributed generation in electricity grids especially for photovoltaic cells, production of wind power, fuel cells and super capacitors, etc. (Xu *et al*., 2013).

Micro-grids are introduced by existence of distributed generation in electricity distribution grids. As the technologies of small industries and production units increase, the influence of micro-grids on energy saving devices aimed at supporting for the transient state speeds up. Micro-grids based on distributed generation are considered as powerful and effective grid backups. In fact, they are one of the most important future trends of power systems (Xu *et al*., 2013).

Currently not only the energy production technologies have advanced but also more attentions are being paid to environmental issues and simultaneously an increasing trend is rising towards optimization of reliability of electricity grids. Furthermore, the necessary motivation for transformation of distribution grids from passive states to active is already created along with tendency for production of renewable energies at distribution system levels. On the other hand, connection of distributed generation sources to current grids is not able to satisfy the entire technical and economic needs of investors. This is while it was expected to observe an improvement in quality of power along with increase of influence and development of distributed generation. Since, there were fluctuations resulting from difference in voltage and frequencies of different renewable energy sources, the expected results were never realized.

Conventional and independent connection of each distributed generation source to the distribution grid leaves undesirable dynamic effects on grid behavior. On this basis, the optimal solution would be creation of small grids which are independent from the main grid. These small grids are called micro-grids. They develop suitable smart controllers and increase network's and grid's reliability and security. Therefore, these micro-grids can provide the contexts for reduction of blackout for consumers.

A micro-grid is a low-voltage power grid that includes a set of local sensitive loads, power supplies, distributed generation and devices used for saving electric energy (Adhikari and Li, 2014). In summary, it can be stated that through a suitable management and controlling DGs and ESSs and loads in a small geographic area, a small grid is shaped which is named as Micro-grid. In fact now a days, the importance of using the former is felt more than ever before (Moradi *et al*., 2016).

The generation units used in micro-grids are called micro-sources (Rahbarimagham *et al*., 2015). Micro-sources include generation units such as Micro-turbines, fuel cells, internal combustion engines, renewable productions (wind and solar power plants) and etc. in addition, electric cars, batteries and super capacitors are usually used in micro-grids as energy saving systems (Ma *et al*., 2014). Figure 1 shows the schematics of configuration of a micro-grid.

Main advantages of the proposed controller over the conventional controllers are its simplicity, speed and precision. Methods that make use of artificial intelligence manifestations such as neural networks, decision making trees and etc. are extremely complicated, require a huge amount of time and data and are therefore less desirable. The advantage of the proposed method over the methods based on artificial intelligence is mainly its simplicity and ease of implementation. The proposed method is in addition, more reliable compared to conventional methods mainly because in the former controller, the PID controller

coefficients are implemented through a simple fuzzy logic that doesn't require training. In fact with only one single implementation, it is able to act in different situations including neutralization of faults.

Designing and implementing PID controllers aimed at neutralization of faults in backup control requires several adjustments and decision makings regarding values or coefficients of PID controller. Adjustment of these coefficients is a difficult task and currently there are several rules and approaches proposed regarding it.

Previous methods adjust coefficients for one load and the values remain constant during the entire consumption cycle. These methods are basically simple and are usually based on empirical relations. However, these methods have one primary problem which is inconsistency of coefficients. This results in reduced responsiveness quality in special occasions. On this basis usually it is inevitable to perform a total review on performance of these types of controllers. There are also other methods proposed in this domain which are based on trainable methods such as neural networks and decision making trees. Among the defects of these methods, the following points could be referred to:

- Lack of existence of specific rules or design guides for designing and adjusting the controller
- Lack of existence of a general method for detection of internal operations of grid
- Extremely hard or even in some cases impossible training

One of the most efficient existing methods for neutralization of faults in backup controls is to design a PID controller with online approaches which determine the values of parameters of the PID controller at each specific time with regard to conditions. Designing and adjusting the coefficients of the PID controller through fuzzy logic is based on deduction strength of fuzzy systems which consider a specific recommendation for values of PID controller's coefficients at each time point. This approach is some sort of scheduling for benefiting from an interest. In fact the task of determination of values of interests is with a fuzzy system. This fuzzy system receives the fault and its derivative at each time point and recalculates the values of coefficients of the PID controller and places them in the controller structure.

MATERIALS AND METHODS

Suggested fuzzy logic PID controller: Previous simulation studies on power systems show that the classic PID controllers have high overshoots and long setting times. In addition more time is required for optimization of control parameters in classic PID controllers and this is while control parameters can't be specific (Yu and Luan, 2015). Mehrian studied vibration response of the intelligent structure (consisting peizoeectric members) (Nowruzpour Mehrian *et al*., 2014; Vaziri *et al*., 2015).

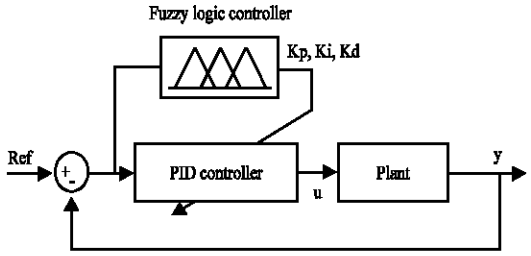

Fig. 2: Overall PID fuzzy controller diagram block

We know that fuzzy systems are basically systems based on knowledge or rules. The heart of a fuzzy system is a database consisted of if-then rules. The schematic of the overall diagram of PID fuzzy control is shown in Fig. 2. In our PID controller, the inputs are EF (error of frequency) and EP (Error of Power) and the (Kp), (Ki) and (Kd) coefficients are the outputs. In general, the equations related to PID controllers can be written as follows:

$$G(s) = Kp + \frac{Ki}{s} + Kds \quad (1)$$

Through taking factors, we will have:

$$G(s) = Kp\,(1 + \frac{1}{Tis} + Tds) \quad (2)$$

We also know that:

$$Ki = \frac{Kp}{Ti},\ Kd = Kp \times Td \quad (3)$$

In order to further simplify the number of unknowns, one can act as follows:

$$Kp,\ Ki,\ Kd \rightarrow Kp',\ Kd',\ \alpha \quad (4)$$

$$\alpha = \frac{Ti}{Td},\ Ki = \frac{Kp^2}{\alpha \times Kd} \quad (5)$$

Instead of elaborating on three coefficients, we will elaborate on two coefficients with a similar effort rate. In order to normalize:

$$Kp' = \frac{Kp - Kp^{min}}{Kp^{max} - Kp^{min}} \rightarrow \in [0,1] \quad (6)$$

$$Kd' = \frac{Kd - Kd^{min}}{Kd^{max} - Kd^{min}} \rightarrow \in [0,1] \quad (7)$$

In Ziegler-Nichols method, the value of $\alpha = 4$ and in fuzzy logics its value is variable between Eq. 2 and 5. We normalize Kp' and Kd' in order to make them independent from the system and adopt a value between 0 and 1. In general, it can be stated that we normalize them in order to make them all-purpose. Through making use of the Mamdany deduction machine the controller is developed and designed. In addition it should be pointed out that designing systems through fuzzy methods is different with respect to problem type, parameters and problem situation. Figure 3 shows the general state of undertaken phases. The following presents the block designed in MATLAB Software along with a short description.

Investigation of simulation blocks: Frequency and power fault inputs are first compared with a reference value and then prepared and moved towards the fuzzy controller according to previously stated descriptions that included applying fuzzy logics, determination of rules, deduction and removal of fuzzy logics. The outputs of the fuzzy block include Proportional coefficients (Kp), Integration coefficients (KI) and Derivative coefficients (Kd). The system applies coefficients on blocks and calculated the value of PREF. The voltage of the three-phase grid is transformed into PREF through the PLL and ABC to DQO transformations (Fig. 4).

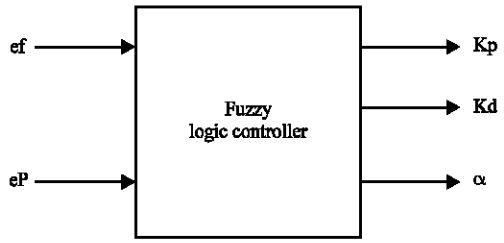

Fig. 3: Inputs and outputs of the fuzzy system

Simulation of inverter's central control: After that the three-phase voltage enters the voltage measurement block, it is directed towards the sub-system related to generation of reference voltage and afterwards is used for production of pulses of PWM gate. In addition, the three-phase is used for the rectifier block of IGBT for production of DC voltage (Fig. 5).

Inverter switching phase (intermediate between DC and AC phases): The specifications and details of the sub-system block shown in the upper figure are manifested in Fig. 6. With respect to this sub-system, after receiving the reference power signal from the central control phase, a switching appropriate for receiving the current from DC phase must take place. In this phase, first the power signal is received along with current and voltage signals and ultimately, DQO is transformed into ABC and therefore the reference voltage is produced. Afterwards, the value is compared with the suitable reference value and after that the fault value is passed through a PI controller; it is redirected towards the

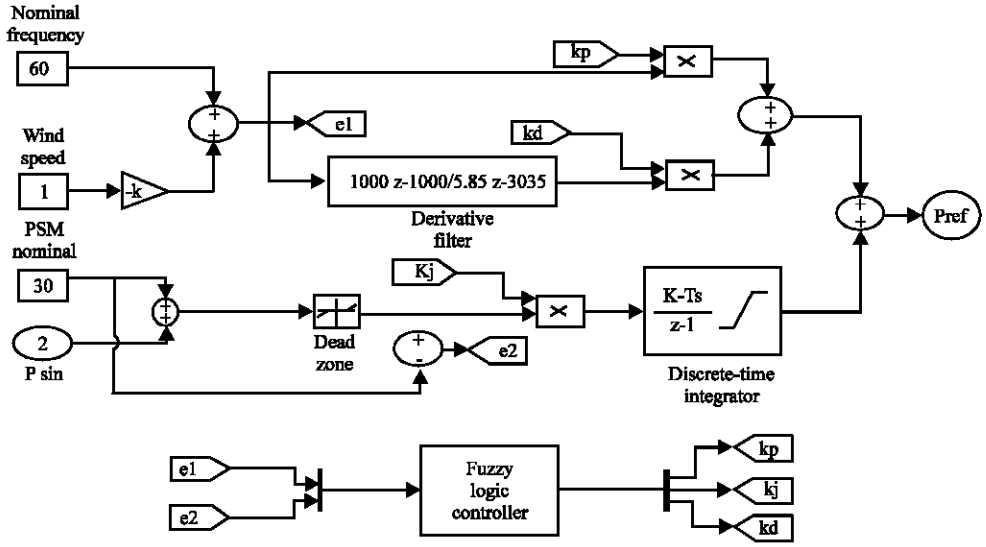

Fig. 4: Schematics of the designed controller

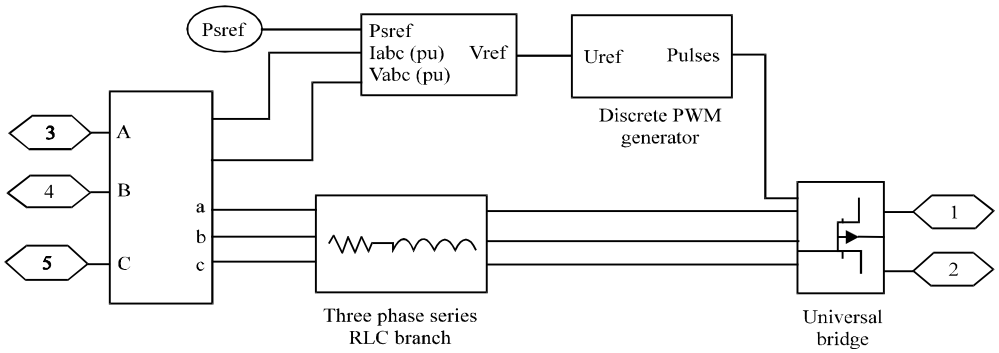

Fig. 5: Overall schematics of the PWM block control

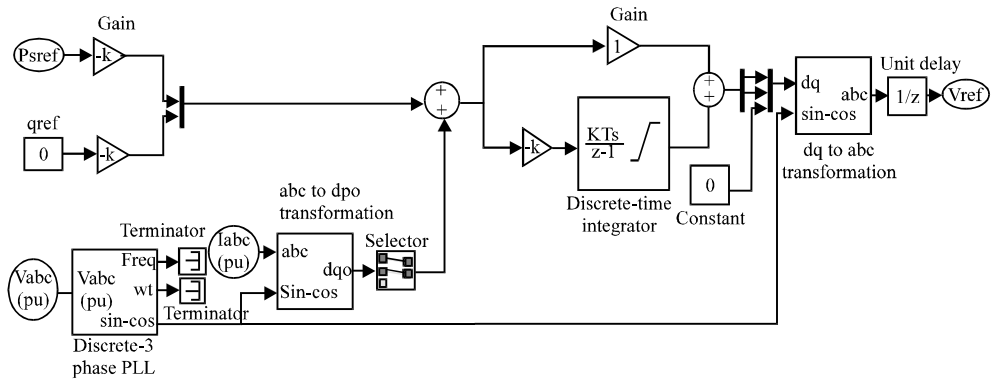

Fig. 6: Block simulate for reference voltage

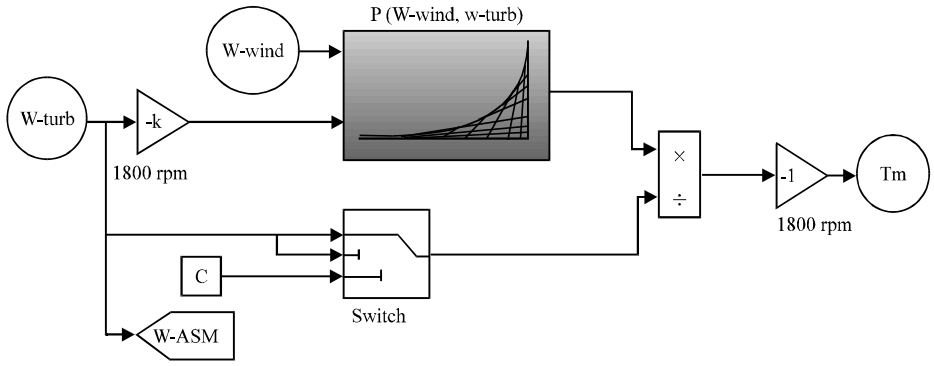

Fig. 7: Diagram block of wind turbine model

reference phase of the ABC frame. Afterwards, the reference voltage value for supplication of the PWM is used for production of fire pulse for switching in power inverters. Therefore, the required pulses are produced and these pulses are then transferred into a diode panel and resultantly switching between AC and DC is performed. In order to overcome the harmonic switching, a filter was used and the output of the filter enters the energy saving system (Nowruzpour Mehrian and Naei, 2013). Figure 6 presents the related simulated block.

Turbine modeling: The inputs of this block are w-wind and W-turbine. According to the output chart, the power chart is received and considering the ratio of P and Angular speed (W), the TM output torque is sent towards the machine for production of electric energy. The diagram block of the wind turbine model is shown in Fig. 7.

Battery modeling: The following block used for modeling of battery. The type of battery used in NI-CD (Fig. 8).

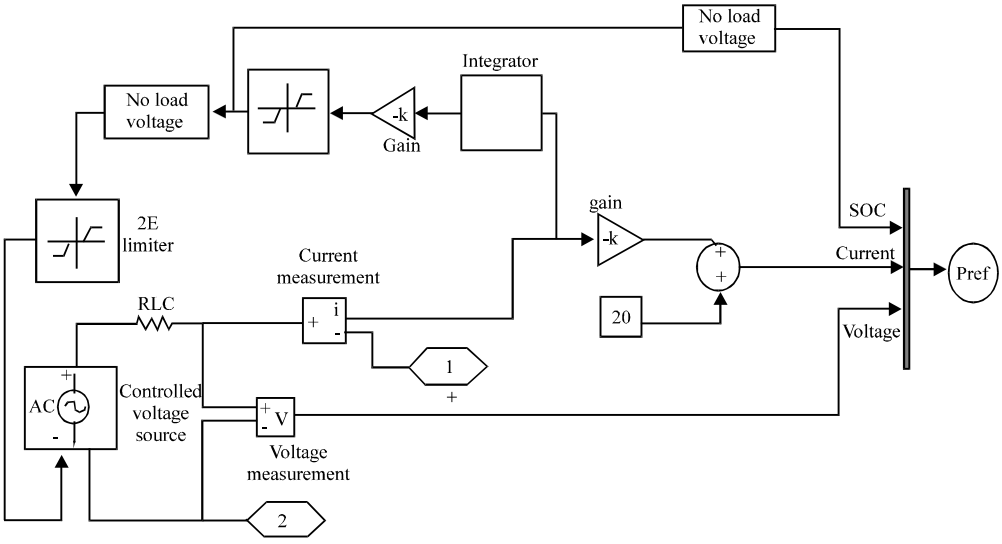

Fig. 8: Modeling of battery in simulink

RESULTS AND DISCUSSION

The system under study: Figure 9 shows the structure of a 480 V micro-grid with two distributed generation sources. The studies system includes a Diesel generator with capacity of 300 KVA, a wind driven turbine with a 270 KVA generator and a 50 Kw NI-CD battery. It should be pointed out that the battery is connected to the primary reference system. The index of power of the wind turbine is shown in Fig. 10. With respect to this index, with a wind speed of 10 m/s the power is approximately <0.8 per unit which is almost 200 kWs. The Simulink environment of the MATLAB Software was used for simulation of the proposed method and investigation of performance of the battery in micro-grid as well (Fig. 11).

Simulation results: In order to evaluate the proposed system, four scenarios have been considered. The first scenario is related to isolation of the micro-grid from the upper grid and the remaining three scenarios are related to island states. These three scenarios include abrupt increase and decrease of load as well as changes in wind speed. The following discusses the results of each scenario.

Microgrid islanded mode: In state of connectivity of micro-grid and the upper grid, the system maintains a suitable stability. If the micro-grid's frequency and voltage are based per units, the production capacity of the generator will be 140 kWs and the wind turbine's production will be 200 kWs at a wind speed f 10 m sec^{-1} The amount of loads of the micro-grid is equal

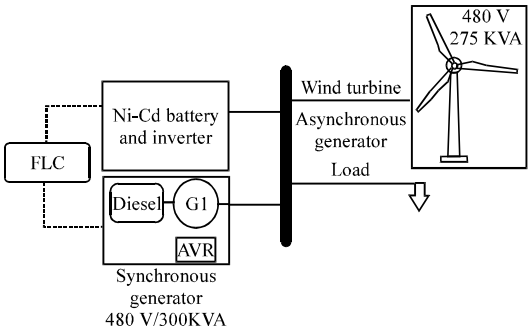

Fig. 9: The schematics of the system under study

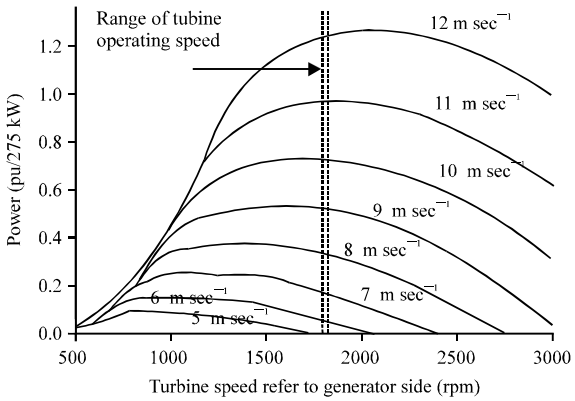

Fig. 10: Wind turbine's power index

to 300 kWs and considering that the entire production of the micro-grid is used for charging, the battery's voltage will be approximately 100 V and its current is

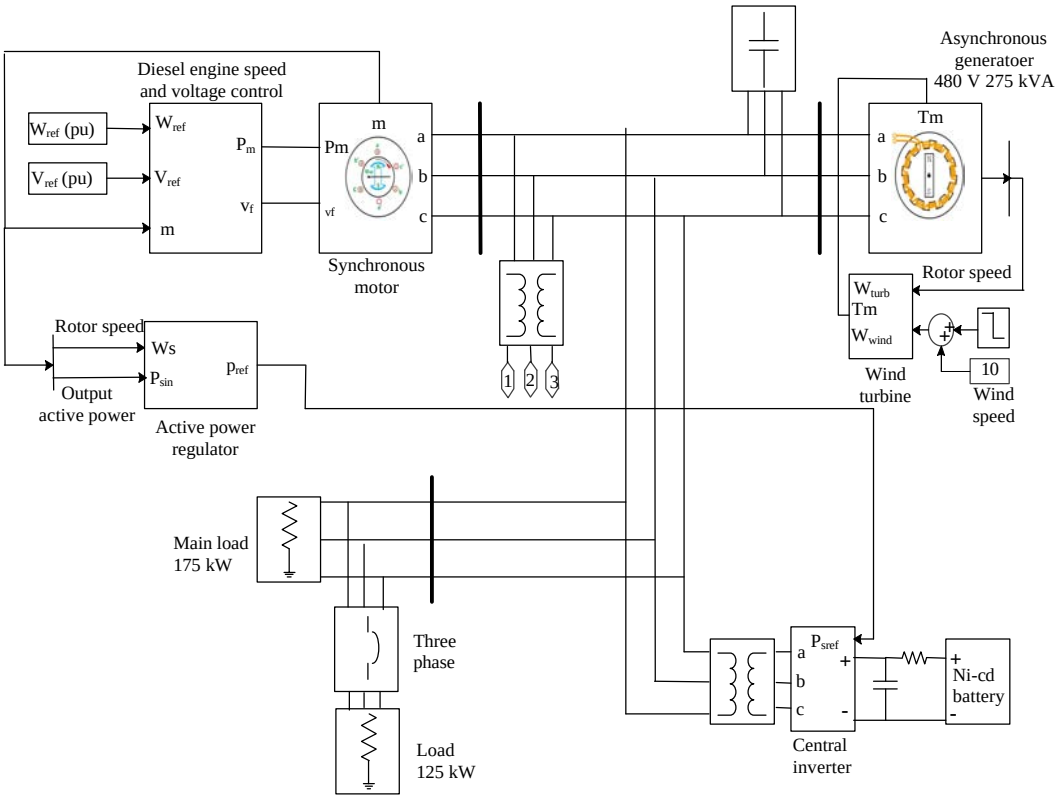

Fig. 11: Simulated system

approximately 250 A. At the tenth moment the micro-grid is isolated from the upper grid. In this situation the task of creating balance between active and reactive powers is with the micro-grid and its designed controllers. The simulation results are shown in Fig. 12-17. At the moment of isolation, the battery is discharged for about 0.5 sec. Figure 12 shows the DC current of the battery. Since that this current is negative, then it can be concluded that the battery was discharged. Micro-grid voltage and frequency parameters are shown in Fig. 13 and 14. As it can be observed, frequency and voltage are respectively accompanied by a very small overshoot (0.005 per unit) and also a very small voltage (0.05 per unit). The reason is that the battery was discharged and that the grid was unable to inject power into the upper grid. At the very first moment of isolation the battery started to discharge in order to maintain the power balance of the micro-grid through increasing the inertia. Afterwards, the generator should produce power proportional to requirement of the micro-grid.

By taking a look at Fig. 15 it can be seen that the production rate of the generator has declined from 140-90 kWs in order to remove the overproduction. The wind speed has remained constant at 10 m sec^{-1}.

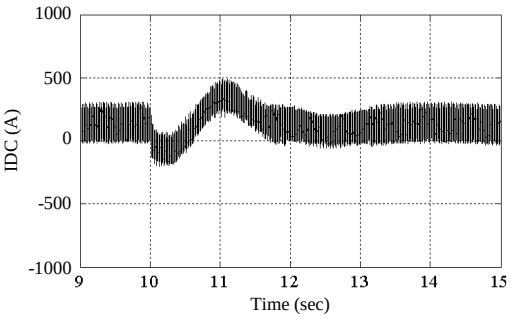

Fig. 12: Current related to the battery

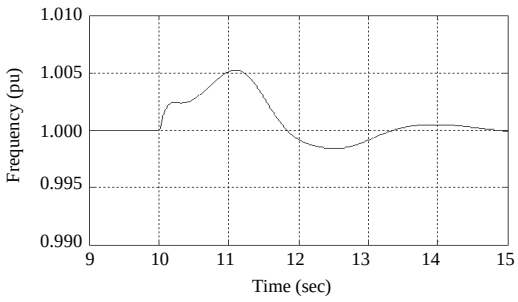

Fig. 13: Micro-grid's frequency based on per-unit

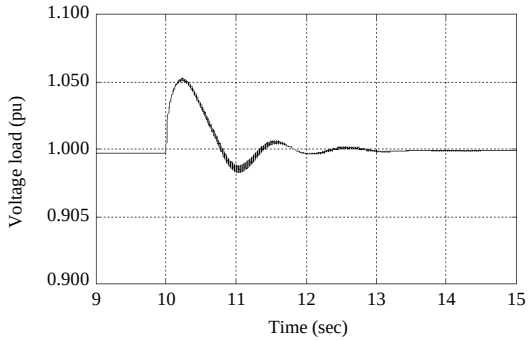

Fig. 14: Micro-grid's voltage based on per-unit

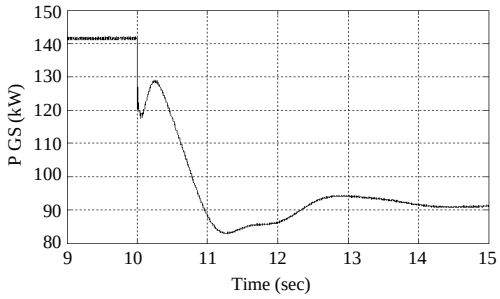

Fig. 15: Active power production ability of the generator

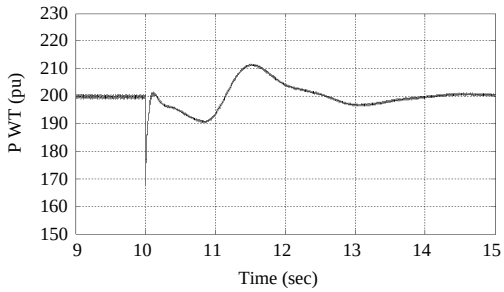

Fig. 16: Production power of the wind turbine at wind speed of 10 m sec^{-1}

therefore, thr production strength of the wind turbine has remained 200 kWs even after fluctuation. The power production ability of the wind turbine is shown in Fig. 16. Figure 17 is related to the micro-grid's consumption. The sum of production ability of the micro-grid after fluctuations resulting from isolation is <300 kWs and the consumption remains still.

The cause of fluctuation is high rate of consumption at the moment of isolation and is related to load dynamics and grid voltage. In general, the battery increases the inertia of the micro-grid and injects power into the micro-grid. Results of simulation indicated the ability of the micro-grid in terms of stability and strength against becoming an island.

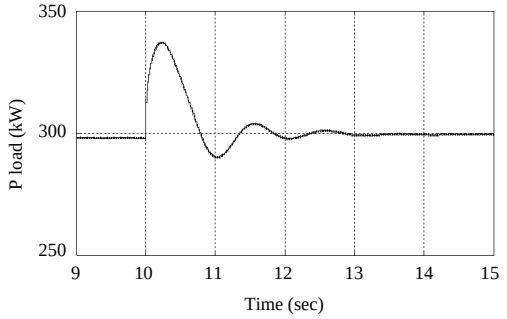

Fig. 17: Active power of electric loads

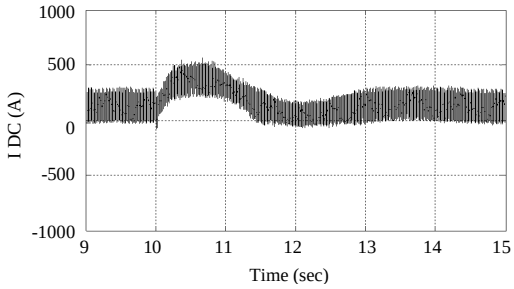

Fig. 18: Battery's DC current

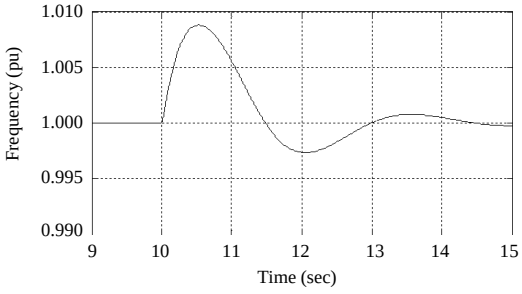

Fig. 19: Micro-grid's frequency per unit

Abrupt decrease of load in Island state: In this scenario, the consumed load is reduced from 325-250 kWs in a gradual state. The 75 kWs reduction occurs at the tenth second of simulation in state of grid independent mode. Moment prior to execution of the scenario, the values of frequency and voltage are equal to 1 per unit, the generator's production capacity is equal to 125 kWs and the production capacity of the wind turbine is equal to approximately 200 kWs. Wind speed is 10 m sec^{-1}. The simulation results regarding this scenario are shown in Fig. 18-23.

With respect to Fig. 18 showing the battery's DC current, it can be observed that with abrupt output of load, the battery absorbs the overproduction of the micro grid and starts charging. Average increase of the DC

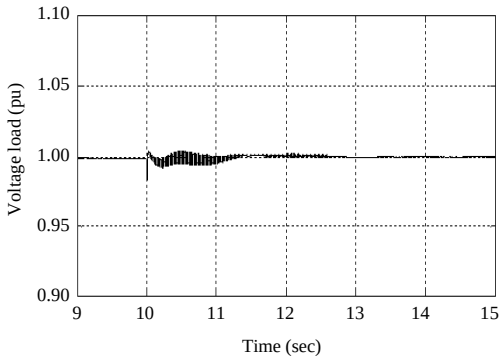

Fig. 20: Micro-grid's voltage per unit

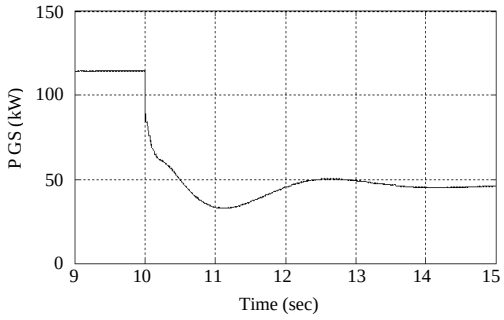

Fig. 21: Active production capacity of generator

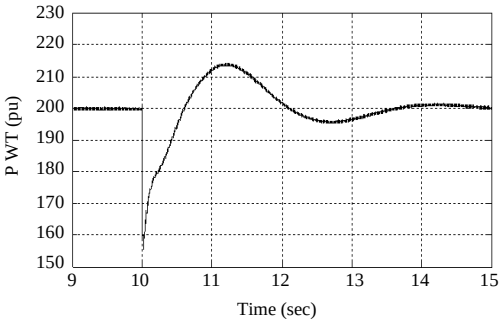

Fig. 22: Active production capacity of wind turbine at wind speed of 10 m sec^{-1}

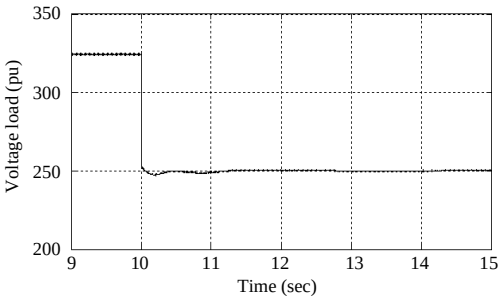

Fig. 23: Active capacity of electrical loads

current up to 500 A is a testimony to this fact. Figures 19 and 20 are respectively related to frequency and voltage of the micro-grid. The overshoot in micro-grid's frequency shows overproduction after abrupt output of load. Frequency fluctuation is in standard range and after fluctuation it has returned to the same primary value of 1 per unit. In addition the Micro-grid's voltage has remained constant at 1 per unit.

The production capacity of the generator is shown in Fig. 21. The production capacity of this generator is reduced from 125-50 kWs in order to maintain the balance of active capacity. After fluctuations, the production capacity of the wind turbine has also remained constant at 200 kWs (Fig. 22). This is because wind speed has remained constant. In general, the micro-grid's production capacity was 325 kWs before execution of the scenario but afterwards, it has declined to 250 kWs. Figure 23 shows the consumption of the micro-grid. The battery absorbs the power of the micro-grid and creates a balance on active capacity in micro-grid. After battery's reaction, the governor of the generator reduces the amount of production and creates a capacity balance. Results of this scenario indicate that the battery backs up the stability of micro-grid.

Abrupt increase of load in Island state: In this scenario, the consumed load is increased from 300-425 kWs in a gradual state. The 125 kWs increase occurs at the tenth second of simulation in state of grid independent mode. Moment prior to execution of the scenario, the values of frequency and voltage are equal to 1 per unit, the generator's production capacity is equal to 90 kWs and the production capacity of the wind turbine is equal to approximately 200 kWs. Wind speed is 10 m sec^{-1}. The simulation results regarding this scenario are shown in Fig. 24-29.

Figure 24 shows the battery's DC current. By taking a look at this figure it can be concluded that as the load abruptly increases, the battery injects the micro-grid's missing capacity and discharges. Negativity of the DC current for approximately up to 500 A shows this issue. Figures 25 and 26 are respectively, related to micro-grid's frequency and voltage. Undershoot observed in the frequency of the micro-grid indicates lack of production after abrupt load increase. Frequency fluctuations are in normal range and the frequency value has returned to its primary value of 1 after fluctuation. In addition the micro-grid's voltage has remained constant at 1. The production capacity of the generator is shown in Fig. 27. The production capacity of the generator has risen from 75-200 kWs in order to maintain the active capacity

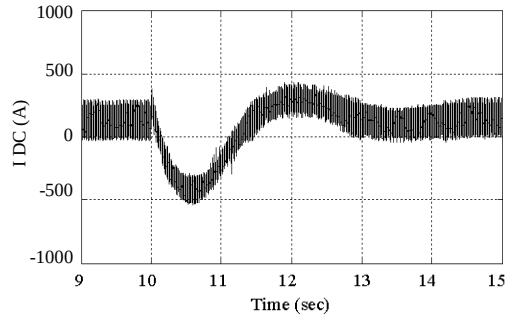

Fig. 24: Battery's DC current

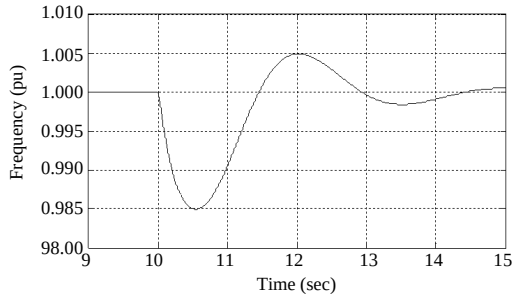

Fig. 25: Micro-grid's frequency per unit

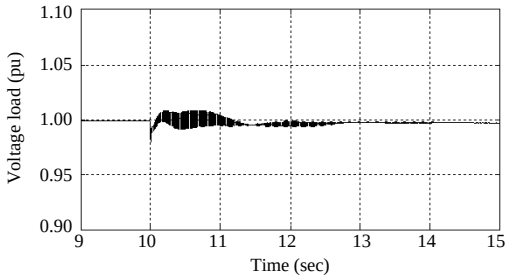

Fig. 26: Micro-grid's voltage per unit

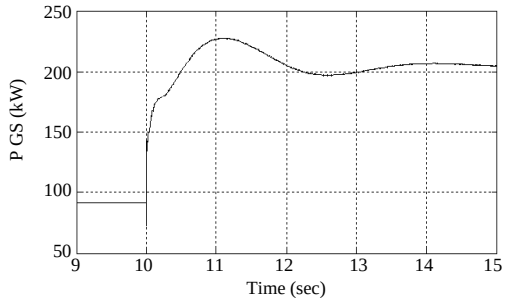

Fig. 27: Generator's active production capacity

balance. After fluctuations, the production capacity of the wind turbine has also remained constant at 200 kWs (Fig. 28). This is because wind speed has remained

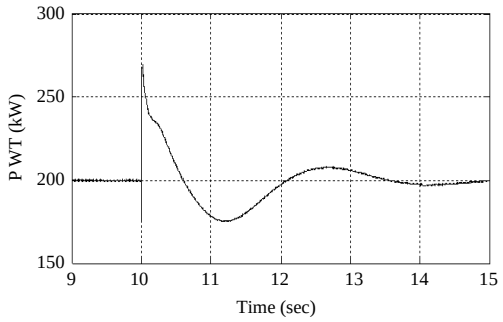

Fig. 28: Production capacity of wind turbine at wind speed of 10 m sec^{-1}

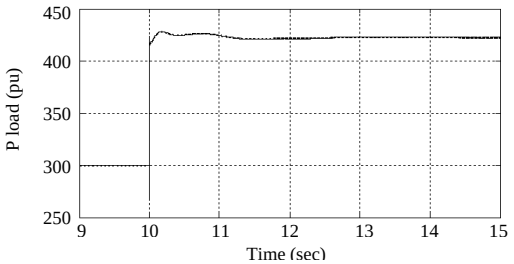

Fig. 29: Active capacity rate of electrical loads

constant. In general, the micro-grid's production capacity was 3200 kWs before execution of the scenario but afterwards it has declined to 425 kWs. Figure 29 shows the consumption of the micro-grid.

In general, the battery injects the power into the micro-grid and therefore maintains the active capacity balance during the initial moments of occurrence of fault. Results of this scenario indicate that the battery backs up the stability of micro-grid.

Wind speed change scenario: In this scenario, at moment 10 the wind speed is reduced from 10-8 m sec^{-1}. Before this scenario the voltage and frequency values were equal to 1 per unit, the production capacity of the generator was equal to 90 kWs and the production capacity of the wind turbine was 200 kWs. The simulation results related to this scenario are shown in Fig. 30-35.

Figure 30 shows the DC current of the battery. This figure shows that as the win speed is decreased, the battery injects the required power for the micro-grid and discharges. Negativity of the DC current for up to 400 A shows this fact. Figures 31 and 32 are respectively related to micro-grid's frequency and voltage. Undershoot observed in the frequency of the micro-grid indicates lack of production after decrease in wind speed. Frequency fluctuations are in normal range and the frequency value

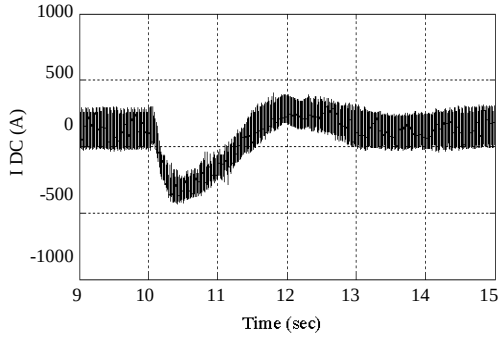

Fig. 30: Battery's DC current

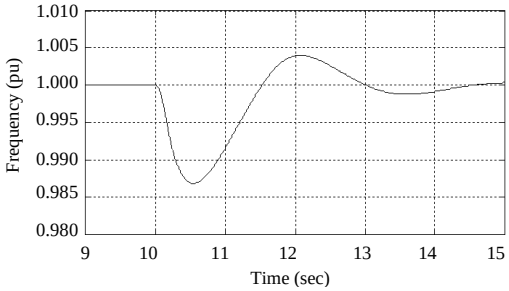

Fig. 31: Micro-grid's frequency per unit

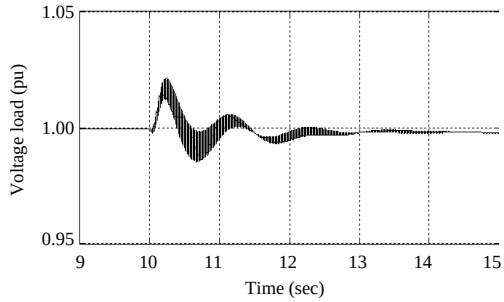

Fig. 32: Micro-grid's voltage per unit

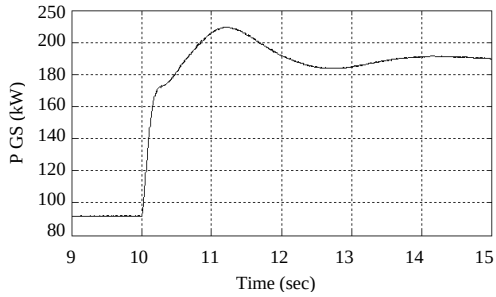

Fig. 33: Active production capacity of generator

has returned to its primary value of 1 after fluctuation. In addition the micro-grid's voltage has remained constant at 1 per unit. The production capacity of the generator has risen from 90-190 kWs in order to maintain the active capacity balance (Fig. 33). The production capacity of the

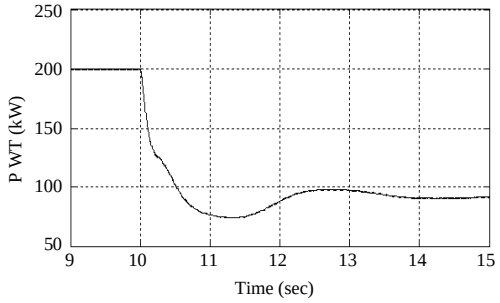

Fig. 34: Production capacity of wind turbine at wind speed of 8 m sec^{-1}

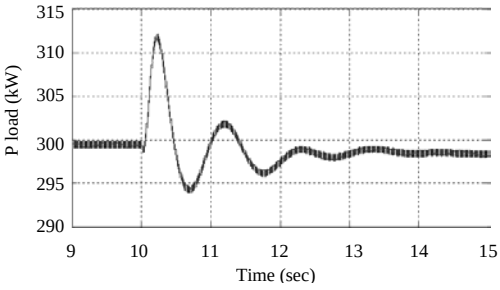

Fig. 35: Active capacity of electrical loads

wind turbine has declined from 200-90 kWs. Figure 34 shows the production capacity index of wind turbine as 0.3 per unit. This value is correct and Fig. 35 shows the consumption of the micro-grid.

CONCLUSION

With respect to investigated and studied scenarios, it can be concluded that making use of energy saving ources in micro-grids aimed at controlling voltage and frequency result in increased overall inertia of the micro-grid and in terms of island mode, it can be accompanied with increased stability. This is mainly because in island mode, it is the micro-grid's task to control voltage and frequency. In this research, we have been able to maintain frequency and voltage in their allowed range under different scenarios. This indicates the appropriateness and validity of our controller in this context. Analysis of data and the simulation results reveal that PID fuzzy controllers have higher speed and precision for neutralization of faults.

REFERENCES

Adhikari, S. and F. Li, 2014. Coordinated Vf and PQ control of solar photovoltaic generators with MPPT and battery storage in microgrids. IEEE. Trans. Smart Grid, 5: 1270-1281.

Gheitaghy, A.M., B. Takabi and M. Alizadeh, 2014. Modeling of ultrashort pulsed laser irradiation in the cornea based on parabolic and hyperbolic heat equations using electrical analogy. Intl. J. Mod. Phys. C., 25: 1-17.

Gudarzi, M., 2015. Synthesis controller design for seismic alleviation of structures with parametric uncertainties. J. Low Freq. Noise Vibr. Active Control, 34: 491-511.

Gudarzi, M., E. Hossein and R. Mostafa, 2015. A general-purpose framework to simulate musculoskeletal system of human body: Using a motion tracking approach. Comput. Methods Biomech. Biomed. Eng. Ahead Print, 2015: 1-14.

Hu, J., J. Zhu, D.G. Dorrell and J.M. Guerrero, 2014. Virtual flux droop method: A new control strategy of inverters in microgrids. IEEE. Trans. Power Electron., 29: 4704-4711.

Ma, Y., P. Yang, Y. Wang, S. Zhou and P. He, 2014. Frequency control of islanded microgrid based on wind-PV-diesel-battery hybrid energy sources. Proceedings of the 17th International Conference on Electrical Machines and Systems (ICEMS) 2014, October 22-25, 2014, IEEE, China, ISBN:978-1-4799-5163-5, pp: 290-294.

Magham, H.R., M.J. Sanjari, B. Zaker and G.B. Gharehpetian, 2012. Voltage profile improvement in a microgrid including PV units using genetic algorithm. Proceedings of the 2nd Iranian Conference on Smart Grids (ICSG) 2012, May 24-25, 2012, IEEE, Tehran, Iran, ISBN:978-1-4673-1399-5, pp: 1-5.

Mahmoud, M.S., S.A. Hussain and M.A. Abido, 2014. Modeling and control of microgrid: an overview. J. Franklin Inst., 351: 2822-2859.

Mehrian, S.M., A. Nazari and M.H. Naei, 2014. Coupled thermoelasticity analysis of annular laminate disk using laplace transform and galerkin finite element method. Appl. Mech. Mater., 656: 298-304.

Mehrian, S.M.N. and S.Z. Mehrian, 2015. Modification of space truss vibration using piezoelectric actuator. Applied Mech. Mater., 811: 246-252.

Mehrian, S.Z., S.R. Amrei, M. Maniat and S.M. Nowruzpour, 2016. Structural health monitoring using optimising algorithms based on flexibility matrix approach and combination of natural frequencies and mode shapes. Intl. J. Struct. Eng., 7: 398-411.

Moradi, M.H., M. Eskandari and S.M. Hosseinian, 2016. Cooperative control strategy of energy storage systems and micro sources for stabilizing microgrids in different operation modes. Intl. J. Electr. Power Energy Syst., 78: 390-400.

Nowruzpour Mehrian, S.M. and M.H. Naei, 2013. Tow dimensional analysis of functionally graded partial annular disk under radial thermal shock using hybrid Fourier-Laplace transform. Applied Mech. Mater., 436: 92-99.

Nowruzpour Mehrian, S.M., M.H. Naei and S.Z. Mehrian, 2013. Dynamic response for a functionally graded rectangular plate subjected to thermal shock based on LS theory. Applied Mech. Mater., 332: 381-395.

Oveisi, A., M. Gudarzi and S.M. Hasheminejad, 2014. Dynamic response of a thick piezoelectric circular cylindrical panel: An exact solution. Shock Vibr., 2014: 1-8.

Rahbarimagham, H., E.M.A. Miri, B. Vahidi, G.B. Gharehpetian and M. Abedi, 2015. Superior decoupled control of active and reactive power for three-phase voltage source converters. Turk. J. Electr. Eng. Comput. Sci., 23: 1025-1039.

Seyedalipour, S.S. and J. Adabi, 2016. An active control technique for integration of distributed generation resources to the power grid. Intl. J. Electr. Power Energy Syst., 77: 353-359.

Takabi, B. and H. Shokouhmand, 2015. Effects of al 2 O 3-Cu/water hybrid nanofluid on heat transfer and flow characteristics in turbulent regime. Intl. J. Mod. Phys. C., 26: 1-25.

Takabi, B. and S. Salehi, 2014. Augmentation of the heat transfer performance of a sinusoidal corrugated enclosure by employing hybrid nanofluid. Adv. Mech. Eng., 2014: 1-16.

Takabi, B., 2016. Thermomechanical transient analysis of a thick-hollow FGM cylinder. Eng. Solid Mech., 4: 25-32.

Takabi, B., A.M. Gheitaghy and P. Tazraei, 2016. Hybrid water-based suspension of Al2O3 and Cu nanoparticles on laminar convection effectiveness. J. Thermophys. Heat Transfer, 30: 523-532.

Vaziri, M.R., S.N. Mehrian, M.H. Naei and J.Y.S. Ahmad, 2015. Modification of shock resistance for cutting tools using functionally graded concept in multilayer coating. J. Thermal Sci. Eng. Applic., Vol. 7, No. 1. 10.1115/1.4028982

Xu, Y., Z.H. Shi, J.Q. Wang and P.F. Hou, 2013. Discussion on the factors affecting the stability of microgrid based on distributed power supply. Energy Power Eng., 5: 1344-1346.

Yu, H. and W. Luan, 2015. Coordinated and optimized control of distributed generation integration. Electric Power Research Institute, China.